

Restricted Rotation around the P–C Bond in Metalated Phosphonium Salts: A Variable-Temperature ^1H NMR Study. X-ray Crystal Structures of $[\{\text{AuP}(\text{C}_6\text{H}_{11})_3\}_2\{\mu\text{-C}(\text{PTO}_3)(\text{py-2})\}]\text{ClO}_4$ and $[(\text{AuPPh}_3)_2\{\mu\text{-}\{\text{C}(\text{PPh}_3)(\text{py-2})\}(\text{AuPPh}_3)\}](\text{CF}_3\text{SO}_3)_2$

José Vicente,^{*,†} María-Teresa Chicote,^{*} and María-Cristina Lagunas

Grupo de Química Organometálica,[‡] Departamento de Química Inorgánica, Facultad de Química, Universidad de Murcia, Apartado 4021, Murcia, 30071 Spain

Peter G. Jones^{*,§} and Birte Ahrens

Institut für Anorganische und Analytische Chemie, Technische Universität Braunschweig, Postfach 3329, 38023 Braunschweig, Germany

Received March 28, 1997[⊗]

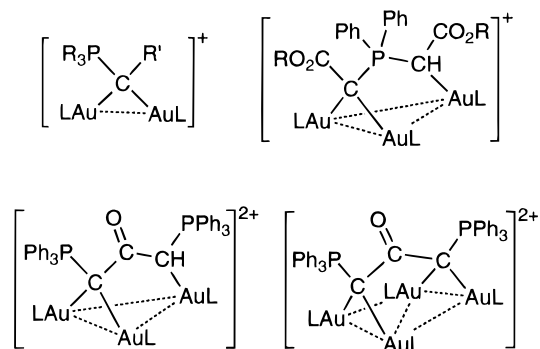
A variable-temperature ^1H NMR study has been performed for the complexes $[(\text{AuL})_2\{\mu\text{-C}(\text{PTO}_3)\text{R}\}]\text{ClO}_4$ [To = $\text{C}_6\text{H}_4\text{Me-4}$; L = PPh_3 , R = $\text{C}(\text{O})\text{NMe}_2$, pyridyl-2 (py-2), $\text{C}(\text{O})\text{Ph}$, $\text{C}(\text{O})\text{C}_6\text{H}_4\text{OMe-4}$, $\text{C}(\text{O})\text{C}_6\text{H}_4\text{NO}_2\text{-4}$, CO_2Me , CN; R = py-2, L = $\text{P}(\text{C}_6\text{H}_4\text{OMe-4})_3$, $\text{P}(\text{C}_6\text{H}_{11})_3$, PMe_3], $[(\text{AuPPh}_3)_2\{\mu_2\text{-}\{\text{C}(\text{PTO}_3)(\text{py-2})\}\{\text{Ag}(\eta^2\text{-O}_2\text{NO})\text{-}(\text{OCIO}_3)\}\cdot\text{H}_2\text{O}$, and $[(\text{AuPPh}_3)_2\{\mu_2\text{-}\{\text{C}(\text{PTO}_3)(\text{py-2})\}(\text{AuPPh}_3)\}](\text{ClO}_4)_2$. The $\text{TO}_3\text{P-C}(\text{AuL})_2$ rotation is shown to be restricted at room or lower temperatures. The estimated values of ΔG^* for these processes lie in the range $67.3\text{--}42.2\text{ kJ}\cdot\text{mol}^{-1}$ and are attributed mainly to steric effects, although electronic effects could also be operative. The crystal structures of $[\{\text{AuP}(\text{C}_6\text{H}_{11})_3\}_2\{\mu\text{-C}(\text{PTO}_3)(\text{py-2})\}]\text{ClO}_4$ (**2c**) and $[(\text{AuPPh}_3)_2\{\mu\text{-}\{\text{C}(\text{PPh}_3)(\text{py-2})\}(\text{AuPPh}_3)\}](\text{CF}_3\text{SO}_3)_2$ (**9'**, $2\text{CH}_2\text{Cl}_2$) have been determined. **2c** crystallizes in the monoclinic system, space group $P2_1/n$, with $a = 14.056(3)\text{ \AA}$, $b = 24.556(4)\text{ \AA}$, $c = 19.110(3)\text{ \AA}$, $\beta = 111.00(2)^\circ$ and $Z = 4$. **9'** crystallizes in the monoclinic system, space group $P2_1/c$, with $a = 17.232(6)\text{ \AA}$, $b = 25.800(7)\text{ \AA}$, $c = 18.005(7)\text{ \AA}$, $\beta = 96.77(3)^\circ$, and $Z = 4$.

Introduction

Many interesting gold(I) complexes show weak attractive inter- and intramolecular $\text{Au(I)}\cdots\text{Au(I)}$ interactions.^{1–3} For example, hypercoordinated complexes such as $[\text{C}(\text{AuL})_6]^{2+}$, $[\text{C}(\text{AuL})_5]^+$, $[\text{RC}(\text{AuL})_4]^+$, $[\text{N}(\text{AuL})_5]^{2+}$, $[\text{P}(\text{AuL})_5]^{2+}$, $[\text{RP}(\text{AuL})_4]^{2+}$, or $[\text{P}(\text{AuL})_6]^{3+}$ (L = triaryl- or trialkylphosphine), prepared by Schmidbaur,^{1,4–6} owe their stability to such weak interactions.⁷ The tendency of the AuL units to form aggregates is termed “aurophilicity”⁵ and has been suggested to arise in part from relativistic effects.⁸

We have reported a series of di-, tri-, and tetranuclear gold(I) complexes with carbonyl-stabilized phosphorus ylides (see Chart 1).^{9–15} Several crystal structures show one or two carbon atoms that bridge two AuL units with short aurophilic

Chart 1



$\text{Au}\cdots\text{Au}$ contacts [$2.862(1)\text{--}3.078(1)\text{ \AA}$].^{9,11–13,15} This interaction narrows the Au-C-Au angles to values [$85.9(7)\text{--}91.1(6)^\circ$] far smaller than expected for sp^3 hybrid orbitals. The P–C bond distances [$1.753(11)\text{--}1.783(14)\text{ \AA}$] are intermediate between the standard $\text{C}(\text{sp}^3)\text{--PR}_3$ bond distance in phosphonium

[†] E-mail: jvs@fcu.um.es.

[‡] WWW: <http://www.scc.um.es/gi/gqo/>.

[§] E-mail: jones@xray36.anchem.nat.tu-bs.de.

[⊗] Abstract published in *Advance ACS Abstracts*, August 1, 1997.

- (1) Schmidbaur, H. *Gold Bull.* **1990**, 23, 11.
- (2) Schmidbaur, H. *Chem. Soc. Rev.* **1995**, 391.
- (3) Jones, P. G. *Gold Bull.* **1981**, 14, 159, 102; **1983**, 16, 114; **1986**, 19, 46.
- (4) Scherbaum, F.; Grohmann, A.; Müller, G.; Schmidbaur, H. *Angew. Chem., Int. Ed. Engl.* **1989**, 28, 463. Grohmann, A.; Riede, J.; Schmidbaur, H. *Nature* **1990**, 345, 140.
- (5) Scherbaum, F.; Grohmann, A.; Huber, B.; Krüger, C.; Schmidbaur, H. *Angew. Chem., Int. Ed. Engl.* **1988**, 27, 1544.
- (6) Schmidbaur, H. *Pure Appl. Chem.* **1993**, 65, 691. Zeller, E.; Schmidbaur, H. *J. Chem. Soc., Chem. Commun.* **1993**, 69 and references therein.
- (7) Häberlein, O. D.; Schmidbaur, H.; Rösch, N. *J. Am. Chem. Soc.* **1994**, 116, 8241.
- (8) Pyykkö, P. *Chem. Rev.* **1988**, 88, 563. Pyykkö, P.; Desclaux, J. P. *Acc. Chem. Res.* **1979**, 12, 276. Görling, A.; Rösch, N.; Ellis, D. E.; Schmidbaur, H. *Inorg. Chem.* **1991**, 30, 3986.

(9) Vicente, J.; Chicote, M. T.; Cayuelas, J. A.; Fernandez-Baeza, J.; Jones, P. G.; Sheldrick, G. M.; Espinet, P. *J. Chem. Soc., Dalton Trans.* **1985**, 1163.

(10) Vicente, J.; Chicote, M. T.; Saura-Llamas, I.; Turpin, J.; Fernandez-Baeza, J. *J. Organomet. Chem.* **1987**, 333, 129.

(11) Vicente, J.; Chicote, M. T.; Lagunas, M. C.; Jones, P. G. *J. Chem. Soc., Dalton Trans.* **1991**, 2579.

(12) Vicente, J.; Chicote, M. T.; Lagunas, M. C. *Inorg. Chem.* **1993**, 32, 3748.

(13) Vicente, J.; Chicote, M. T.; Saura-Llamas, I.; Jones, P. G.; Meyer-Bäse, K.; Erdbrügger, C. F. *Organometallics* **1988**, 7, 997.

(14) Vicente, J.; Chicote, M. T.; Saura-Llamas, I. *J. Chem. Soc., Dalton Trans.* **1990**, 1941.

(15) Vicente, J.; Chicote, M. T.; Lagunas, M. C.; Jones, P. G. *J. Chem. Soc., Chem. Commun.* **1991**, 1730.

Scheme 1

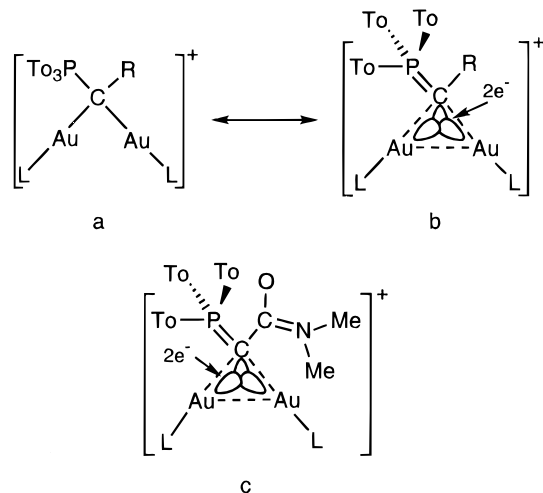
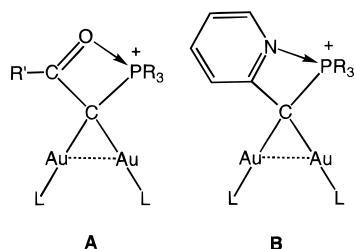


Chart 2



salts [1.787(4)¹⁶ – 1.893(8) Å¹³] and that found in the related carbonyl-stabilized ylide Ph₃P=C(C₆F₄CN-4)CO₂Et [1.722(3) Å].¹⁷ To account for these data, we postulated that the bonding in these species could be described as being a hybrid between the resonance forms **a**, a diaurated phosphonium salt, and **b**, an ylidic form, in which a three-center two-electron bond is responsible for the bonding interaction in the CAu₂ moiety, and the remaining p(α-C) orbital forms a pπ(α-C)→dπ(P) bond (see Scheme 1).⁹ All the above-mentioned crystal structures also display X–P distances [where X is the oxygen atom in the C(O)R (R = OMe, OEt, Me, Ph, NMe₂) moieties or the N atom in the pyridyl-2 group (see **A** and **B** in Chart 2)] short enough [2.73 – 2.92 Å] to allow some pπ(X)→dπ(P) interaction.

In an attempt to obtain new data for the latter interaction and/or the multiple-bond character of the P–CAu₂ bond in such species, we carried out a variable-temperature ¹H NMR study on a series of complexes [(AuL)₂{μ-C(PTO₃)R}]ClO₄ (To = C₆H₄Me-4). We found the rotation of PTO₃ around the α-C–P bond to be restricted at room or lower temperatures in all these complexes.

Experimental Section

IR spectroscopy, elemental analyses, conductance measurements, melting point determinations, and NMR spectroscopy were carried out as described elsewhere.¹⁸ Unless otherwise stated, NMR spectra were recorded in CDCl₃ on a Varian Unity 300, at room temperature. Chemical shifts are referred to TMS (¹H) or H₃PO₄ [³¹P{¹H}]. The complex [(AuP(pmp))₂{μ-C(PTO₃)(py-2)}]ClO₄ (**2b**) (pmp = C₆H₄OMe-4) was described previously.¹²

[(AuL)₂{μ-C(PTO₃)R}]ClO₄ [To = C₆H₄Me-4; L = PPh₃, R = C(O)NMe₂ (**1**), pyridyl-2 (**2a**), C(O)Ph (**3**), C(O)C₆H₄OMe-4

(**4**), C(O)C₆H₄NO₂-4 (**5**), CO₂Me (**6**), CN (**7**); L = P(C₆H₄OMe-4)₃ = P(**pmp**)₃, R = py-2 (**2b**)]. To a solution of the corresponding phosphonium salt, [To₃PCH₂R]ClO₄, in acetone (**1**, **3**–**7**) or dichloromethane (**2a**, **b**) was added an excess of [Au(acac)L] [1:3 (**2a**, **3**–**7**), 1:8 (**2b**)]. The resulting suspension was stirred [96 h (**1**), 38 h (**2a**), 24 h (**2b**, **7**), 20 h (**3**), 22 h (**4**), 16 h (**5**), 44 h (**6**)] in the air (**2a**, **b**, **3**, **4**, **6**, **7**) or under N₂ (**1**, **5**) and filtered over Celite. The solution was concentrated (2 mL) and diethyl ether (20 mL) added to precipitate the desired product, [(AuL)₂{μ-C(PTO₃)R}]ClO₄, as an off-white solid, which was recrystallized from dichloromethane–diethyl ether, washed with diethyl ether, and air-dried. **1** was also dried in an oven at 80 °C.

[(AuPPh₃)₂{μ-C(PTO₃)C(O)NMe₂}]ClO₄ (**1**). Yield: 44%. Anal. Calcd for C₆₁H₅₇Au₂ClNO₅P₃: C, 52.09; H, 4.08; N, 0.99; Au, 28.01. Found: C, 51.88; H, 4.21; N, 0.98; Au, 28.12. Mp: 195 °C (dec). Λ_M = 129 Ω⁻¹·mol⁻¹·cm² (3.4 × 10⁻⁴ mol·L⁻¹). IR: ν(CO) 1550 cm⁻¹. NMR: ¹H (60 °C) 2.35 [s br, 9H, Me (To)], 3.31 (s, 6H, MeN), 7.1–7.5 (m, 42H, Ph) ppm; ¹H (20 °C) 2.15 [s, 3H, Me (To)], 2.47 [s, 6H, Me (To)], 3.34 (s br, 6H, MeN), 6.5–8 (m, 42H, Ph) ppm; ¹H (–40 °C) 2.16 [s, 3H, Me (To)], 2.51 [s, 6H, Me (To)], 2.98 (s, 3H, MeN), 3.79 (s, 3H, MeN), 6.4–8 (m, 42H, Ph) ppm; ³¹P{¹H} 30.49 (s, PTO₃), 37.57 (s, PPh₃) ppm. Figure 1 gives the ¹H NMR variable-temperature study of complex **1**.

[(AuPPh₃)₂{μ-C(PTO₃)(py-2)}]ClO₄ (**2a**). Yield: 87%. Anal. Calcd for C₆₃H₅₅Au₂ClNO₄P₃: C, 53.57; H, 3.92; N, 0.99; Au, 27.89. Found: C, 53.16; H, 4.43; N, 0.99; Au, 28.12. Mp: 180 °C (dec). Λ_M = 116 Ω⁻¹·mol⁻¹·cm² (2.5 × 10⁻⁴ mol·L⁻¹). NMR: ¹H (20 °C) 2.37 (s br, 9H, Me), 6.64 [m, 1H, H5 (py)], 7.1–8.0 (m, 45H, To + Ph + py) ppm; ¹H (–40 °C) 2.18 (s, 3H, Me), 2.49 (s, 6H, Me), 6.5–7.9 (m, 46H, To + Ph + py) ppm; ³¹P{¹H} 31.08 (s, CPTO₃), 36.93 (d, AuPPh₃) ppm.

[(AuPPh₃)₂{μ-C(PTO₃)C(O)Ph}]ClO₄ (**3**). Yield: 76%. Anal. Calcd for C₆₅H₅₆Au₂ClNO₅P₃: C, 52.24; H, 3.92; Au, 27.37. Found: C, 54.23; H, 3.95; Au, 27.03. Mp: 279 °C (dec). Λ_M = 108 Ω⁻¹·mol⁻¹·cm² (5.2 × 10⁻⁴ mol·L⁻¹). IR: ν(CO) 1547 cm⁻¹. NMR: ¹H (40 °C) 2.35 (s br, 9H, Me), 7.3–8.4 (m, 47H, Ar) ppm; ¹H (–60 °C) 2.22 (s, 3H, Me), 2.54 (s, 6H, Me), 6.7–8.8 (m, 47H, Ar) ppm; ³¹P{¹H} 30.84 (s, PTO₃), 37.41 (s, PPh₃) ppm.

[(AuPPh₃)₂{μ-C(PTO₃)C(O)(C₆H₄OMe-4)}]ClO₄ (**4**). Yield: 54%. Anal. Calcd for C₆₆H₅₈Au₂ClNO₆P₃: C, 53.94; H, 3.98; Au, 26.81. Found: C, 53.91; H, 3.94; Au, 27.27. Mp: 209 °C (dec). Λ_M = 104 Ω⁻¹·mol⁻¹·cm² (4.2 × 10⁻⁴ mol·L⁻¹). IR: ν(CO) 1544 cm⁻¹. NMR: ¹H (50 °C) 2.39 [s br, 9H, Me (To)], 3.82 (s, 3H, MeO), 6.6–8.6 (m, 46H, Ar) ppm; ¹H (–60 °C) 2.21 [s, 3H, Me (To)], 2.54 [s, 6H, Me (To)], 3.92 (s, 3H, MeO), 6.6–8.7 (m, 46H, Ar) ppm; ³¹P{¹H} 31.28 (s, PTO₃), 37.52 (s, PPh₃) ppm.

[(AuPPh₃)₂{μ-C(PTO₃)C(O)(C₆H₄NO₂-4)}]ClO₄ (**5**). Yield: 90%. Anal. Calcd for C₆₅H₅₅Au₂ClNO₇P₃: C, 52.59; H, 3.73; N, 0.94; Au, 26.54. Found: C, 52.28; H, 3.79; N, 0.80; Au, 26.21. Mp: 130 °C. Λ_M = 115 Ω⁻¹·mol⁻¹·cm² (43.8 × 10⁻⁴ mol·L⁻¹). IR: ν(CO) 1582 cm⁻¹. NMR: ¹H (20 °C) 2.45 (s br, 9H, Me), 7–8.4 (m, 46H, Ar) ppm; ¹H (–60 °C) 2.23 (s, 3H, Me), 2.56 (s, 6H, Me), 6.7–8.7 (m, 46H, Ar) ppm; ³¹P{¹H} 30.14 (s, PTO₃), 37.51 (s, PPh₃) ppm.

[(AuPPh₃)₂{μ-C(PTO₃)CO₂Me}]ClO₄ (**6**). Yield: 89%. Anal. Calcd for C₆₀H₅₄Au₂ClO₆P₃: C, 51.72; H, 3.91; Au, 28.27. Found: C, 51.31; H, 4.20; Au, 27.92. Mp: 121 °C (dec). Λ_M = 110 Ω⁻¹·mol⁻¹·cm² (5 × 10⁻⁴ mol·L⁻¹). IR: ν(CO) 1644 cm⁻¹. NMR: ¹H (20 °C) 2.38 [s br, 9H, Me (To)], 3.59 (s, 3H, MeO), 7.2–7.7 (m, 42H, Ph + To) ppm; ¹H (–40 °C) 2.29 [s, 3H, Me (To)], 2.59 [s, 6H, Me (To)], 3.64 (s, 3H, MeO), 6.6–8 (m, 42H, Ph + To) ppm; ³¹P{¹H} 31.29 (s, PTO₃), 37.17 (s, PPh₃) ppm. Figure 1 gives the ¹H NMR variable-temperature study of complex **6**.

[(AuPPh₃)₂{μ-C(PTO₃)CN}]ClO₄·H₂O (**7**). Yield: 91%. Anal. Calcd for C₅₉H₅₃Au₂ClNO₅P₃: C, 51.41; H, 3.87; N, 1.02; Au, 28.58. Found: C, 50.98; H, 3.85; N, 1.06; Au, 29.16. Mp: 215 °C (dec). Λ_M = 125 Ω⁻¹·mol⁻¹·cm² (5 × 10⁻⁴ mol·L⁻¹). IR: ν(CN) 2158 cm⁻¹. NMR: ¹H 1.66 (s, 2H, H₂O), 2.43 (s, 9H, Me), 7.1–7.8 (m, 42H, Ph) ppm; ¹H (–95 °C, Cl₂CD₂) 2.34 (s, 3H, Me), 2.57 (s, 6H, Me), 6.8–8 (m, 42H, Ph) ppm; ³¹P{¹H} 32.79 (t, PTO₃, J_{PP} = 6.1 Hz), 36.95 (d, PPh₃) ppm.

[(AuPCy₃)₂{μ-C(PTO₃)(py-2)}]ClO₄ (**2c**). A suspension of [To₃PCH₂(py-2)]ClO₄ (205.3 mg, 0.414 mmol) and [Au(acac)PCy₃] (Cy = C₆H₁₁) (477.3 mg, 0.828 mmol) in acetone (30 mL) was stirred (4 days)

(16) Bram, A.; Burzlaff, H.; Hadawi, D.; Bestmann, H. *Acta Crystallogr., Sect. C* **1993**, *49*, 1409.

(17) Vicente, J.; Chicote, M. T.; Fernandez-Baeza, J.; Fernandez-Baeza, A.; Jones, P. G. *J. Am. Chem. Soc.* **1993**, *115*, 794.

(18) Vicente, J.; Abad, J. A.; Fernandez-de-Bobadilla, R.; Jones, P. G.; Ramirez de Arellano, M. C. *Organometallics* **1996**, *15*, 24.

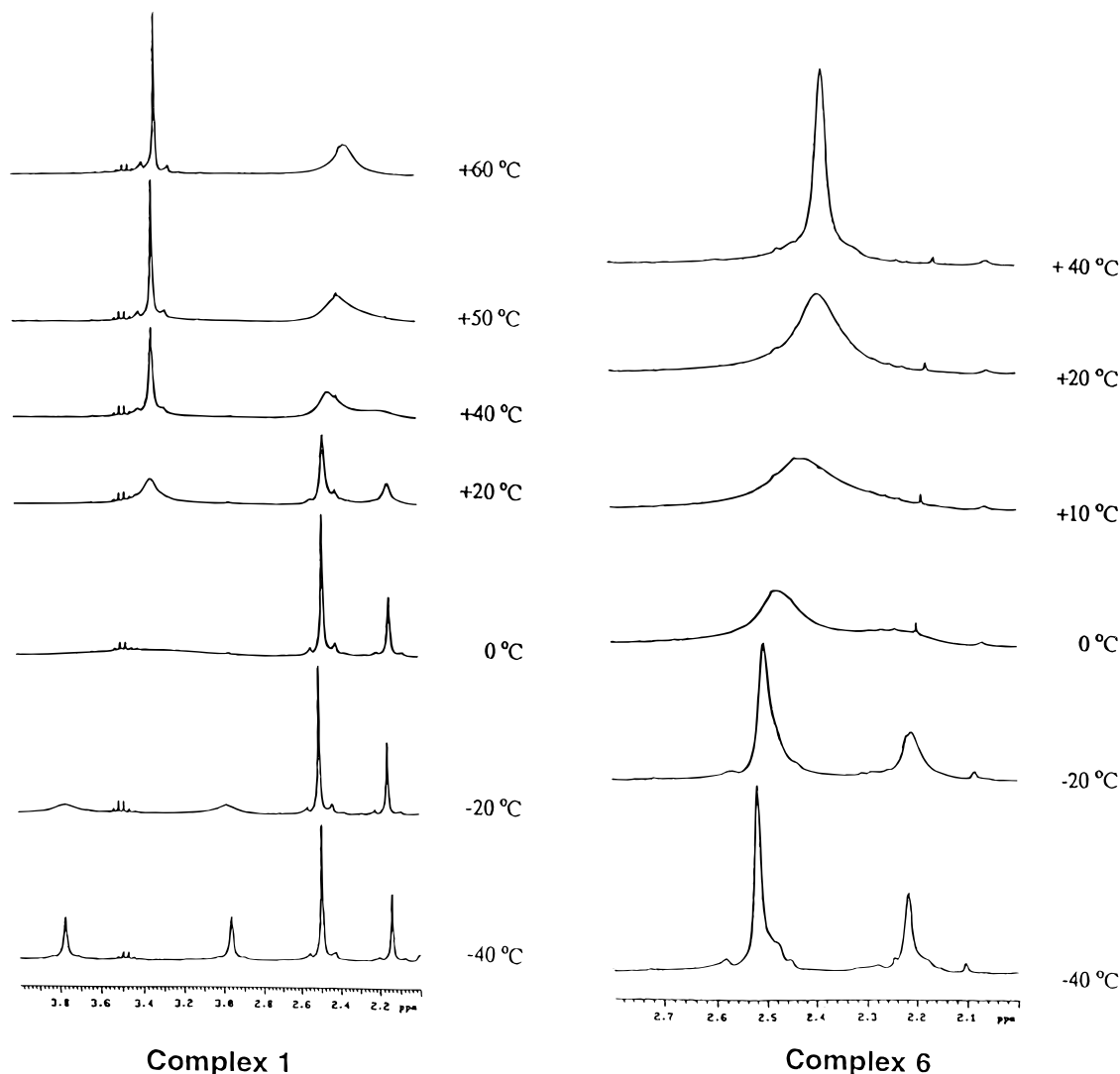


Figure 1. Variable-temperature ^1H NMR spectra of complexes **1** and **6**.

and filtered over Celite. The solution was concentrated (3 mL), and diethyl ether (20 mL) was added to give a suspension, which was filtered. Slow evaporation of the filtrate gave off-white crystals of **2c**. Anal. Calcd for $\text{C}_{63}\text{H}_{91}\text{Au}_2\text{ClNO}_4\text{P}_3$: C, 52.23; H, 6.33; N, 0.97. Found: C, 52.64; H, 6.42; N, 1.03. Mp: 212 °C (dec). $\Lambda_M = 105 \Omega^{-1}\text{mol}^{-1}\text{cm}^2$ ($2 \times 10^{-4} \text{mol}\cdot\text{L}^{-1}$). NMR: ^1H 1.28 (m, 33H, Cy), 1.80 (m, 33H, Cy), 2.40 (s br, 9H, Me), 6.6–7.8 (m, 16H, To + py) ppm; ^1H (-50°C) 1.27 (m, 33H, Cy), 1.80 (m, 33H, Cy), 2.37 (s, 3H, Me), 2.42 (s, 6H, Me), 6.6–7.8 (m, 16H, To + py) ppm; $^{31}\text{P}\{^1\text{H}\}$ 31.35 (s, PTo_3), 56.83 (d, PCy_3) ppm.

Crystallography of 2c. See Figure 2 for the ORTEP diagram of this compound. Tables 1 and 2 give crystallographic data and selected bond lengths and angles. The crystal was mounted in inert oil on a glass fiber and transferred to the cold gas stream of the diffractometer (STOE STADI-4 with a Siemens LT-2 low-temperature device). Data were collected using monochromated Mo $\text{K}\alpha$ radiation to $2\theta_{\text{max}} 50^\circ$. Absorption corrections were based on ψ scans. The structure was solved by the heavy-atom method and refined anisotropically on F^2 (program SHELXL-93, G. M. Sheldrick, University of Göttingen). Rings C(11)–C(16) and C(71)–C(77) were disordered over two positions and were refined isotropically. Hydrogen atoms were included using a riding model. An extensive system of restraints was applied to light-atom displacement parameter components and local ring geometry. Other data: independent reflections, 10 809; parameters, 649; restraints, 849; $S(F^2)$, 1.065; maximum $\Delta\rho$, $0.96 \text{ e}\ \text{\AA}^{-3}$.

[{Au(PMe₃)₂}₂{ μ -C(PTo₃)(py-2)}]ClO₄ (2d**).** To a solution of [AuCl(PMe₃)₂] (287.7 mg, 0.932 mmol) in acetone (30 mL) was added Ti(acac) (367.8 mg, 1.212 mmol). The resulting suspension was stirred for 16 h and evaporated to dryness, and the residue was extracted with

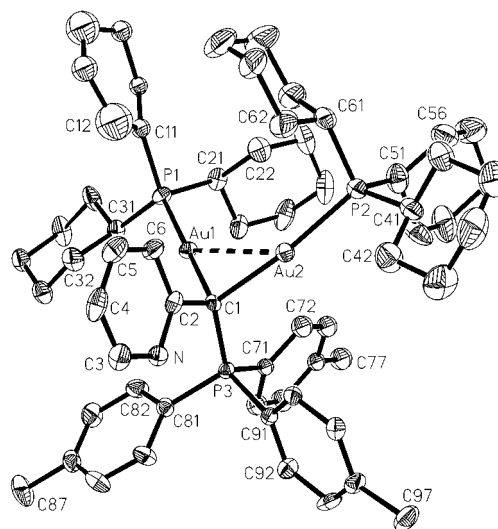


Figure 2. ORTEP diagram of complex **2c** showing the atom labeling. Ellipsoids are drawn at the 50% probability level, and H atoms are omitted for clarity.

a 1:10 mixture of acetone–diethyl ether ($3 \times 40 \text{ mL}$). The extracts were filtered through Celite, and the filtrates were concentrated to dryness. The residue was suspended in 20 mL of acetone, and $[\text{To}_3\text{-PCH}_2(\text{py-2})]\text{ClO}_4$ (115.1 mg, 0.233 mmol) was added to the suspension, which was then stirred for 20 h. The reaction mixture was concentrated to ca. 2 mL, and diethyl ether (20 mL) was added to precipitate **2d** as

Table 1. Crystal Data for Complexes **2c** and **9'**

	2c	9'
mol formula	C ₆₃ H ₉₄ Au ₂ ClNO ₄ P ₃	C ₈₂ H ₆₈ Au ₃ Cl ₄ F ₆ NO ₆ P ₄ S ₂
<i>M_r</i>	1451.68	2198.07
space group	<i>P</i> 2 ₁ / <i>n</i>	<i>P</i> 2 ₁ / <i>c</i>
<i>a</i> (Å)	14.056(3)	17.232(6)
<i>b</i> (Å)	24.556(4)	25.800(7)
<i>c</i> (Å)	19.110(3)	18.005(7)
β (deg)	111.00(2)	96.77(3)
<i>V</i> (Å ³)	6158(2)	7949(5)
<i>Z</i>	4	4
<i>T</i> (K)	143(2)	173(2)
λ (Å)	0.710 73	0.710 73
ρ_{calc} (Mg/m ³)	1.566	1.837
<i>F</i> (000)	2924	4264
μ (mm ⁻¹)	6.588	5.8559
<i>R</i> 1 ^a	0.042	0.052
<i>wR</i> 2 ^b	0.094	0.158

^a $R1 = \sum ||F_o| - |F_c|| / \sum |F_o|$ for reflections with $I > 2\sigma(I)$. ^b $wR2 = [\sum [w(F_o^2 - F_c^2)^2] / \sum [w(F_o^2)^2]]^{0.5}$ for all reflections; $w^{-1} = \sigma^2(F^2) + (aP)^2 + bP$, where $P = (2F_c^2 + F_o^2)/3$ and *a* and *b* are constants set by the program.

Table 2. Selected Bond Lengths (Å) and Angles (deg) for Complex **2c**

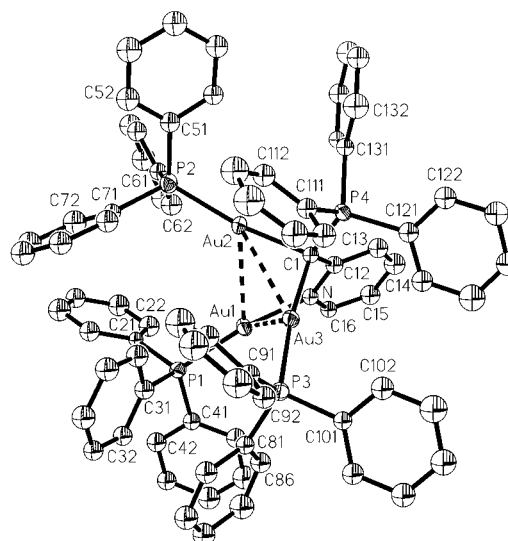
Au(1)–C(1)	2.099(7)	Au(1)–C(1)–Au(2)	90.4(3)
Au(2)–C(1)	2.094(7)	C(1)–Au(1)–P(1)	179.1(2)
Au(1)–Au(2)	2.9757(9)	C(1)–Au(2)–P(2)	172.6(2)
Au(1)–P(1)	2.276(2)	P(3)–C(1)–Au(1)	111.2(3)
Au(2)–P(2)	2.279(2)	P(3)–C(1)–Au(2)	115.5(3)
C(1)–P(3)	1.762(7)	C(2)–C(1)–P(3)	113.5(5)

an off-white solid, which was recrystallized twice from acetone–diethyl ether (1:4). Yield: 20%. Anal. Calcd for C₃₃H₄₃Au₂ClNO₄P₃: C, 38.11; H, 4.17; N, 1.35. Found: C, 38.03; H, 4.34; N, 1.25. Mp: 149 °C (dec). $\Lambda_M = 125 \Omega^{-1} \cdot \text{mol}^{-1} \cdot \text{cm}^2$ ($3.8 \times 10^{-4} \text{ mol} \cdot \text{L}^{-1}$). NMR: ¹H (20 °C) 1.44 (d, 18H, MeP, ²*J*_{PH} = 10 Hz), 2.40 [s, 9H, Me (To)], 6.55 (m, 1H, py), 7.2–7.8 (m, 16H, To + py) ppm; ¹H (–50 °C, Cl₂CD₂) 1.36 (d, 18H, MeP, ²*J*_{PH} = 10 Hz), 2.32 [s, 3H, Me (To)], 2.38 [s, 6H, Me (To)], 6.55 (m, 1H, py), 7.2–7.8 (m, 16H, To + py) ppm; ³¹P{¹H} –1.75 (s, PMe₃), 31.39 (s, PTO₃) ppm.

[(AuPPh₃)₂{ μ -{C(PTO₃)(py-2)}{Ag(η^2 -O₂NO)(OCIO₃)}]}·H₂O (**8**). To a solution of **2a** (328.0 mg, 0.232 mmol) in acetone was added an equimolar amount of AgNO₃. The resulting suspension was stirred for 20 h in the dark and filtered over Celite. The solution was concentrated (1 mL), and diethyl ether was added to precipitate **8** as an off-white solid, which was recrystallized from dichloromethane–diethyl ether. Yield: 86%. Anal. Calcd for C₆₃H₅₇AgAu₂ClN₂O₈P₃: C, 47.28; H, 3.59; N, 1.75. Found: C, 46.88; H, 3.91; N, 1.80. Mp: 153 °C (dec). $\Lambda_M = 137 \Omega^{-1} \cdot \text{mol}^{-1} \cdot \text{cm}^2$ ($4.3 \times 10^{-4} \text{ mol} \cdot \text{L}^{-1}$). NMR: ¹H 1.65 (s, 2H, H₂O), 2.41 (s br, 9H, Me), 6.71 [m, 1H, H3 (py)], 7.1–7.6 (m, 44H, Ph + To + py), 8.31 [m, 1H, H6 (py)] ppm; ¹H (–90 °C, Cl₂CD₂) 2.10 (s, 3H, Me), 2.60 (s, 6H, Me), 6.4–8.5 (m, 46H, Ph + To + py) ppm; ³¹P{¹H} 23.41 (s, PTO₃), 37.35 (s, PPh₃) ppm.

[(AuPPh₃)₂{ μ -{C(PTO₃)(py-2)}(AuPPh₃)}](ClO₄)₂ (**9**). To a solution of **8** (84.1 mg, 0.053 mmol) in acetone was added [AuCl(PPh₃)] (26.2 mg, 0.053 mmol). The resulting suspension was stirred for 1.5 h and filtered over Celite. To the solution was added NaClO₄·H₂O (14.9 mg, 0.106 mmol), and the suspension was stirred for 2.5 h and then concentrated to dryness. The residue was extracted with dichloromethane, the extract filtered through Celite, and the solution concentrated (2 mL). Addition of diethyl ether gave **9** as an off-white solid. Yield: 79%. Anal. Calcd for C₈₁H₇₀Au₃Cl₂NO₈P₄: C, 49.35; H, 3.58; N, 0.71. Found: C, 49.26; H, 3.45; N, 0.84. Mp: 167 °C. $\Lambda_M = 214 \Omega^{-1} \cdot \text{mol}^{-1} \cdot \text{cm}^2$ ($2.3 \times 10^{-4} \text{ mol} \cdot \text{L}^{-1}$). NMR: ¹H (50 °C) 2.41 (s, 9H, Me), 6.6–7.8 (m, 60H, Ph + To + py), 8.60 [m, 1H, H6 (py)] ppm; ¹H (0 °C) 2.28 (s, 3H, Me), 2.51 (s, 6H, Me), 6.6–7.8 (m, 60H, Ph + To + py), 8.60 [m, 1H, H6 (py)] ppm; ³¹P{¹H} 21.84 (s br, N AuPPh₃), 27.66 (s, PTO₃), 36.69 (d, CAuPPh₃, *J*_{PP} = 6.4 Hz) ppm.

[(AuPPh₃)₂{ μ -{C(PPh₃)(py-2)}(AuPPh₃)}](CF₃SO₃)₂·2H₂O (**9'**·2H₂O). To a solution of [(AuPPh₃)₂{ μ -{C(PPh₃)(py-2)}]

**Figure 3.** ORTEP diagram of complex **9'** showing the atom labeling. Ellipsoids are drawn at the 50% probability level, and H atoms are omitted for clarity.**Table 3.** Selected Bond Lengths (Å) and Angles (deg) for Complex **9'**

Au(1)–N	2.090(12)	Au(2)–C(1)–Au(3)	97.2(6)
Au(2)–C(1)	2.120(14)	C(1)–Au(2)–P(2)	171.9(4)
Au(3)–C(1)	2.09(2)	C(1)–Au(3)–P(3)	171.2(4)
Au(1)–Au(2)	3.175(2)	P(4)–C(1)–Au(2)	104.7(7)
Au(2)–Au(3)	3.1570(13)	P(4)–C(1)–Au(3)	107.4(8)
Au(1)–Au(3)	3.0427(12)	P(4)–C(1)–C(12)	116.5(11)
Au(1)–P(1)	2.245(4)	N–Au(1)–P(1)	162.6(4)
Au(2)–P(2)	2.281(4)		
Au(3)–P(3)	2.284(4)		
C(1)–P(4)	1.81(2)		

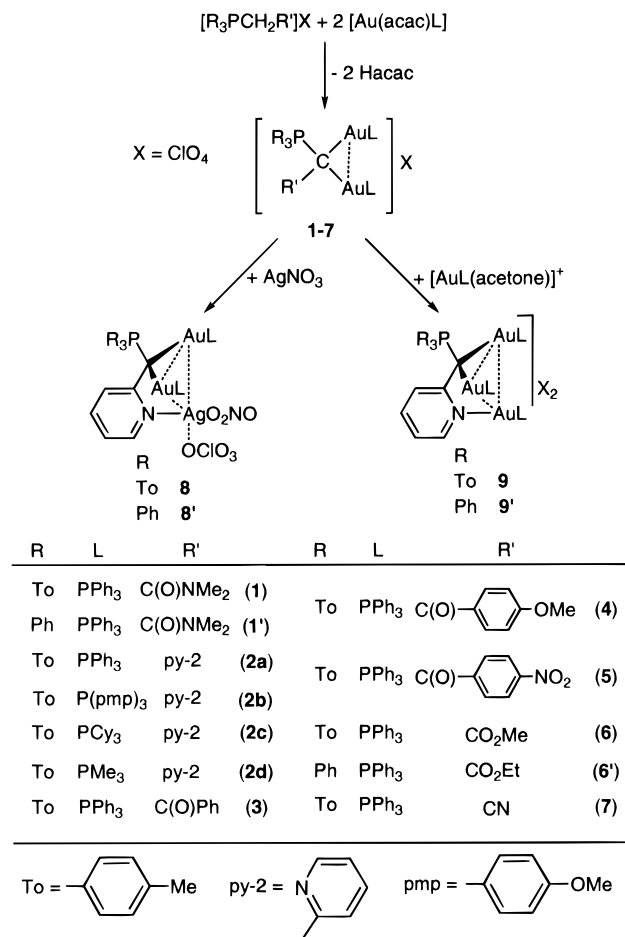
(AuPPh₃)}](ClO₄)₂¹² (107.5 mg, 0.055 mmol) in acetone (20 mL) was added potassium triflate (20.9 mg, 0.112 mmol). The resulting solution was stirred for 1 h and concentrated to dryness, the residue was extracted with dichloromethane (20 mL) and was filtered through Celite, and the solution was concentrated to 2 mL. Upon addition of diethyl ether (30 mL) **9'**·2H₂O precipitated as a white solid which was filtered off and vacuum dried. Single crystals of **9'**·2CH₂Cl₂ suitable for an X-ray diffraction study grew by slow diffusion of diethyl ether into a dichloromethane solution of **9'**. Yield, 84%. Anal. Calcd for C₈₀H₆₈Au₃F₆NO₈P₄S₂: C, 46.55; H, 3.32; N, 0.68. Found: C, 46.92; H, 2.97; N, 0.75. Mp: 146 °C. $\Lambda_M = 237 \Omega^{-1} \cdot \text{mol}^{-1} \cdot \text{cm}^2$ ($1.5 \times 10^{-4} \text{ mol} \cdot \text{L}^{-1}$). NMR: ¹H 1.69 (s, 4H, H₂O), 6.8–7.9 (m, 63H, Ph + py), 8.72 [m, 1H, H6 (py)] ppm; ³¹P{¹H} 22.69 (br, N AuPPh₃), 27.83 (s, CPPH₃), 36.98 (d, CAuPPh₃, ³*J*_{PP} = 5.3 Hz) ppm.

Crystallography of 9'·2CH₂Cl₂. See Figure 3 for the ORTEP diagram of this compound. Tables 1 and 3 give crystallographic data and selected bond lengths and angles. Details are as for **2c**, with the following exceptions: Siemens P4 diffractometer; solution by direct methods; C and N atoms all isotropic; two ordered molecules of dichloromethane in the structure. Other data: independent reflections, 10 418; parameters, 568; restraints, 288; *S*(*F*²), 1.082; maximum $\Delta\rho$, 2.48 e Å⁻³.

Results

Synthesis of Complexes. We have prepared a series of complexes [(AuL)₂{ μ -C(PTO₃)R}]ClO₄ [To = C₆H₄Me-4; L = PPh₃, R = C(O)NMe₂ (**1**), pyridyl-2 (py-2) (**2a**), C(O)Ph (**3**), C(O)C₆H₄OMe-4 (**4**), C(O)C₆H₄NO₂-4 (**5**), CO₂Me (**6**), CN (**7**); R = py-2, L = P(pmp)₃ (**2b**) (pmp = C₆H₄OMe-4), PCy₃ (Cy = C₆H₁₁) (**2c**), PMe₃ (**2d**)] in the same way described for their homologs with PPh₃–*viz.*, by reacting the corresponding

Scheme 2



phosphonium salts $(To_3PCH_2R)ClO_4$ with $[Au(acac)L]$ ^{11,12} (*acacH* = acetylacetonate; see Scheme 2).

The literature synthesis of $[Au(acac)(PPh_3)]$ ¹⁹—reaction of $Tl(acac)$ and $[AuCl(PPh_3)]$ —has been successfully applied to synthesize its homologs with $P(pmp)_3$ and PCy_3 . The reaction between $Tl(acac)$ and $[AuCl(PMe_3)]$ gave the corresponding acetylacetonate–gold(I) complex as an oil, which decomposed after manipulation. Its preparation *in situ* and subsequent reaction with $[To_3PCH_2(py-2)]ClO_4$ gave complex **2d** in 20% yield.

Reactions between $(To_3PCH_2R)ClO_4$ and $[Au(acac)L]$ [$L = PPh_3, P(pmp)_3$] were carried out in 1:3 (**2a,b** and **3–7**) or 1:8 (**1**) molar ratios. Excess of $[Au(acac)L]$ prevented contamination of the digold complexes with the monosubstituted products, $[Au\{\{CH(PTO_3)R\}L\}ClO_4]$.^{11,12} The solubility of $[Au(acac)L]$ [$L = PPh_3, P(pmp)_3$] in 1:10 acetone–diethyl ether or dichloromethane–diethyl ether mixtures allowed its separation from the reaction products. However, when the reaction of $[To_3PCH_2(py-2)]ClO_4$ and $[Au(acac)(PCy_3)]$ was carried out in a 1:3 or 1:5 molar ratio, the excess of the latter was difficult to eliminate. As expected, when the reaction was performed in a 1:2 molar ratio, a mixture of **2c**, $[Au(acac)(PCy_3)]$, and $[Au(PCy_3)\{CH(PTO_3)(py-2)\}]ClO_4$ was obtained. Extraction of the dried mixture with acetone–diethyl ether (1:10) and slow evaporation of the extract gave single crystals of **2c**.

The trinuclear complexes $[(AuPPh_3)_2\{\mu_2-C(PTO_3)(py-2)\}-\{Ag(\eta^2-O_2NO)(OCIO_3)\} \cdot H_2O]$ (**8**) and $[(AuPPh_3)_2\{\mu_2-C(PTO_3)(py-2)\}(AuPPh_3)](ClO_4)_2$ (**9**) were obtained as described for their homologs with PPh_3 (see Scheme 2).¹²

Crystal Structures of Complexes 2c and 9'. The X-ray crystal structure of $[(AuPPh_3)_2\{\mu_2-C(PTO_3)(py-2)\}]ClO_4$ (**2c**) shows features similar to those of other analogous ylide digold(I) compounds $[(AuP(pmp)_3)_2\{\mu_2-C(PTO_3)(py-2)\}]ClO_4$ (**2b**)¹² and $[(AuPPh_3)_2\{\mu_2-C(PPh_3)C(O)NMe_2\}]ClO_4$ (**1'**) (here and below we add a prime to the homologs of **1–9** containing PPh_3 instead of PTO_3).¹¹ Surprisingly, in spite of the bulky phosphine PCy_3 bound to Au(I) in **2c**, the Au(I)⋯Au(I) distance [2.9757 (9) Å] is similar to those of **2b** [2.949 (1) Å] or **1'** [2.938 (1) Å] and lies in the usual range 3.00 ± 0.25 Å found in related complexes.^{1,3} The values of the Au(2)–C(1)–Au(1) angle [90.4 (3)°] and the P(3)–C(1) distance [1.762 (7) Å] in **2c** are also similar to those found in **2b** [88.9(4)°, 1.753(11) Å] or **1'** [88.4(7)°, 1.783(14) Å].

The synthesis of the trigold complex $[(AuPPh_3)_2\{\mu-C(PPh_3)(py-2)\}(AuPPh_3)](ClO_4)_2$ was described previously.¹² Here we report the crystal structure of the analogous triflate complex (**9'**), which we assume to be similar to that of the complex $[(AuPPh_3)_2\{\mu-C(PTO_3)(py-2)\}(AuPPh_3)](ClO_4)_2$ (**9**), studied in this paper. The crystal structure of **9'** reveals that the lone pair of the pyridine group is used to bond a third $AuPPh_3$ moiety and that Au(I)⋯Au(I) short contacts [3.0427(12)–3.175(2) Å] between the three gold atoms are present. The rotation of the pyridine ring (compare structure **B** in Chart 2 and **8** or **9** in Scheme 2) was first observed in the structure of complex **8'**.^{12,15}

Variable-Temperature ¹H NMR of the Complexes. Figure 1 shows the Me region of the ¹H NMR spectra of complexes **1** and **6**, revealing that the singlet observed at room or higher temperatures for the three Me (To) groups splits at low temperatures into two 2:1 singlets (see 2.6–2.1 ppm region in Figure 1). This is a feature common to all complexes **1–9**. Calculated values for the free energy of activation ΔG^{\ddagger} ²⁰ of the P–C torsional processes are given in Table 4 and range from 42.2 to 67.3 (± 0.8) kJ·mol^{−1}. Complexes are ordered in decreasing values of ΔG^{\ddagger} . The differences Δ between ΔG^{\ddagger} of a given complex and that of the next one in the Table 4 are also calculated to facilitate comparisons.

We postulated that the bonding in all these species could be described as a resonance between forms **a** and **b**, in which a three-center two-electron bond is responsible for the bonding interaction in the CAu₂ moiety and the remaining p(α-C) orbital could form a $p\pi(\alpha-C) \rightarrow d\pi(P)$ bond (see Introduction and Scheme 1). In the solid state, the existence of a $p\pi(X) \rightarrow d\pi(P)$ intramolecular interaction [where X is the oxygen atom in **1** or **3–6** (see **A** in Chart 2) or the nitrogen atom in **2** (see **B** in Chart 2)] is a reasonable hypothesis according to the P⋯O and P⋯N distances measured from the crystal structures of **1'** (2.73 Å),¹¹ **2b** (2.82 Å),¹² **2c** (2.85 Å; this work), and **6'** (2.92 Å).⁹ Because these $p\pi(\alpha-C) \rightarrow d\pi(P)$ and $p\pi(X) \rightarrow d\pi(P)$ interactions could explain the restricted rotation of the To_3P group around the P–C bond, we have prepared and studied derivatives with different substituents. Unfortunately, the method required for the synthesis of these complexes (see Scheme 2) does not allow them to be prepared with all possible substituents.

According to Table 4, ΔG^{\ddagger} decreases, for dinuclear complexes containing $AuPPh_3$ or $AuP(pmp)_3$ groups, in the order **1** [$R = C(O)NMe_2$, 65.6 kJ·mol^{−1}] > **3–5** [$R = C(O)(aryl)$, 63.9–59.6 kJ·mol^{−1}] > **2a,b** ($R = py-2$, 58.9–58.5 kJ·mol^{−1}) > **6** ($R = CO_2Me$, 57.7 kJ·mol^{−1}) > **7** ($R = CN$, 42.2); *i.e.*, it is lower when R is more electron-withdrawing and smaller. The higher ΔG^{\ddagger} values are associated with the most sterically demanding L ligand (PCy_3 in **2c**), whereas low ΔG^{\ddagger} values correspond to the smaller R group (CN in **7**) or L ligand (PMe_3 in **2d**). The influence of electronic factors can be judged by

(19) Gibson, D.; Johnson, B. F. G.; Lewis, J. J. *Chem. Soc. A* **1970**, 367.(20) Shanan-Atidi, H.; Bar-Eli, K. H. *J. Phys. Chem.* **1970**, *74*, 961.

Table 4. Calculated²⁰ ΔG^* Values for the P–C Torsional Process in the Complexes [(AuL)₂{ μ -C(PTO₃)R}]ClO₄

	L	R	T _c (K)	$\delta\nu$ (Hz)	ΔG^* (kJ·mol ⁻¹ ± 0.8)	Δ
2c	PCy ₃	py-2	308	16	67.3	1.7
1	PPh ₃	C(O)NMe ₂	323	109	65.6	0.7
9	PPh ₃	py-2(AuPPh ₃)	308	71	64.9	1.0
4	PPh ₃	C(O)(C ₆ H ₄ OMe-4)	313	97	63.9	1.2
3	PPh ₃	C(O)Ph	308	96	62.7	3.1
5	PPh ₃	C(O)(C ₆ H ₄ NO ₂ -4)	293	98	59.6	0.7
2b	P(pmp) ₃	py-2	288	81	58.9	0.4
2a	PPh ₃	py-2	288	94	58.5	0.8
6	PPh ₃	CO ₂ Me	283	94	57.7	0
8	PPh ₃	py-2(AgO ₂ NO)(OCIO ₃)	288	151	57.7	2.0
2d	PMe ₃	py-2	258	21	55.7	13.5
7	PPh ₃	CN	208	70	42.2	

comparing ΔG^* values in complexes **3–5**. The decreasing values (especially for **5**) with increasing electron-withdrawing ability of the R groups could indicate decreasing $p\pi(\alpha\text{-C})\rightarrow d\pi(\text{P})$ bonding, according to our model.

Because the donating ability of the [AuL]₂ moieties should increase with the basicity of the L ligands, one would expect that more basic phosphines would reinforce the $p\pi(\alpha\text{-C})\rightarrow d\pi(\text{P})$ interaction and correspondingly would decrease ΔG^* values in the series **2c** [$pK_a(\text{PCy}_3) = 9.65$]^{21,22} > **2d** [$pK_a(\text{PMe}_3) = 8.65$]²² >> **2b** [$pK_a(\text{P(pmp)}_3) = 4.57$]^{21,23} > **2a** [$pK_a(\text{PPh}_3) = 2.73$].^{21,22} However, the order found is **2c** > **2b** \cong **2a** > **2d**, which can be accounted for in terms of steric hindrance of the phosphines (PCy₃ > PPh₃ > PMe₃).

In order to evaluate the influence of the $p\pi(\text{X})\rightarrow d\pi(\text{P})$ interactions on the restricted rotation of the PTO₃ in solution, we have prepared and studied the trinuclear complexes **8** and **9** (see Scheme 2), in which such interactions are precluded by the coordination of the pyridyl N atom to the third metal atom. Any significant contribution of the P \cdots N interaction in **2a** to the restricted rotation of the PTO₃ moiety in solution can be discarded according to the similar or greater value of ΔG^* obtained for complex **8** or **9**, respectively, with respect to that of **2a** [$\Delta G^*(\mathbf{8}) - \Delta G^*(\mathbf{2a}) = -0.8$ kJ·mol⁻¹; $\Delta G^*(\mathbf{9}) - \Delta G^*(\mathbf{2a}) = 6.4$ kJ·mol⁻¹]. These data also indicate (i) the unobservable effect of the $p\pi(\alpha\text{-C})\rightarrow d\pi(\text{P})$ bonding on the ΔG^* of rotation of the PTO₃ moiety in solution (otherwise, the values of ΔG^* in **8** and **9** should be lower than that of **2a** because coordination of a third metal must remove electron density from the $\alpha\text{-C}$ atom) and (ii) the importance of steric effects shown by the high value of $\Delta G^*(\mathbf{9}) - \Delta G^*(\mathbf{2a})$.

All the above data suggest that the restricted rotation studied is mainly due to steric effects but that some less extensive electronic effects could be operative. Such electronic effects work in the direction predicted by our bonding model (see Scheme 1). Several authors have studied dynamic intramolecular processes of transition metal complexes containing phosphine ligands. They found^{24,25} the ΔG^* values for the torsion about the metal–P bond to range from 36 to 60

kJ·mol⁻¹, the highest values corresponding to the most crowded square planar complexes of Pd or Pt. For the torsion of the substituents at the phosphorus atom about the P–C bond ΔG^* (kJ·mol⁻¹) values of 10–37 are found for PPh₃, 38–40 for PPh(Bu)₂, and 63.6 for P(Mes)₃ (Mes = mesityl). As far as we are aware, only one phosphonium salt [[P(Mes)₃Me]⁺] has been studied, a ΔG^* value of 83.5 kJ·mol⁻¹ being found for the torsion of the mesityl group about the P–C bond.²⁴ From the published data it is apparent that steric rather than electronic factors are dominant in determining barriers to rotation about the P–metal or P–C bonds.

The ¹H NMR spectra of complex **1** (see Figure 1) and the ylide To₃PCHC(O)NMe₂ show, in the range –55 to –80 °C, slow rotation of the NMe₂ group around the N–C(O) bond on the NMR time scale ($\Delta G^* = 52.3$ and 44.7 kJ·mol⁻¹, respectively). This phenomenon is well-known for amides.²⁶ The experimental ΔG^* values lie in the range 45–90 kJ·mol⁻¹.²⁷ This restricted rotation is mainly attributed to the ability of the oxygen atom to polarize the C–O bond, thus increasing the C–N bond order. Indeed, the crystal structure of [(AuPPh₃)₂{ μ -C(PPh₃)C(O)NMe₂}]ClO₄ reveals a short C–NMe₂ bond distance and a planar geometry at nitrogen.¹¹

Conclusions. A variable-temperature ¹H NMR study on a series of di- or trinuclear complexes derived from [To₃PCH₂R]⁺ phosphonium salts shows, for the first time, the rotation of PR₃ around a P–C_{alkyl} bond to be restricted at room or lower temperatures. Although the phenomenon can be mainly attributed to steric effects, the concurrence of minor electronic

(21) Goel, R. G.; Allman, T. *Can. J. Chem.* **1982**, *60*, 716.(22) Streuli, C. A.; Henderson, W. A. *J. Am. Chem. Soc.* **1960**, *82*, 5791.(23) Goetz, H.; Sidhu, A. *Liebigs Ann. Chem.* **1965**, *682*, 71.(24) Bayler, A.; Bowmaker, G. A.; Schmidbaur, H. *Inorg. Chem.* **1996**, *35*, 5959.(25) Bushweller, C. H.; Lourandos, M. Z. *Inorg. Chem.* **1974**, *13*, 2514. Chudek, J. A.; Hunter, G.; MacKay, R. L.; Kremminger, P.; Schlögl, K.; Weissensteiner, W. *J. Chem. Soc., Dalton Trans.* **1990**, 2001. Davies, S. G.; Derome, A. E.; McNally, J. P. *J. Am. Chem. Soc.* **1991**, *113*, 2854. DiMeglio, C. M.; Luck, L. A.; Rithner, C. D.; Rheingold, A. L.; Elcesser, W. L.; Hubbard, J. L.; Bushweller, C. H. *J. Phys. Chem.* **1990**, *94*, 6255. Fanizzi, F. P.; Lanfranchi, M.; Natile, G.; Tiripicchio, A. *Inorg. Chem.* **1994**, *33*, 3331. Howell, J. A. S.; Palin, M. G.; McArdle, P.; Cunningham, D.; Goldschmidt, Z.; Gottlieb, H. E.; Hezroni-Langerman, D. *Inorg. Chem.* **1991**, *30*, 4685. Hunter, G.; Weakley, T. J. R.; Weissensteiner, W. *J. Chem. Soc., Dalton Trans.* **1987**, 1545.(26) Günter, H. *NMR Spectroscopy*; John Wiley & Sons: New York, 1980; p 234 ff.(27) Haushalter, K. A.; Lau, J.; Roberts, J. D. *J. Am. Chem. Soc.* **1996**, *118*, 8891. Wiberg, K. B.; Rablen, P. R.; Rush, D. J.; Keith, T. A. *J. Am. Chem. Soc.* **1995**, *117*, 4261.

effects cannot be neglected. The values of ΔG^* due to the combined influence of steric and electronic effects arising from the substituent attached to the α -C have been found in the range 67.3–42.2 kJ·mol⁻¹. The basicity of the phosphines attached to the gold atoms seems not to affect ΔG^* , whereas their size does have an effect. An increase of 11 kJ·mol⁻¹ in the ΔG^* values is observed when PMe₃ is exchanged for PCy₃. In solution, the influence of the intramolecular $p\pi(X) \rightarrow d\pi(P)$ interactions ($X = N$ in complexes **2**) on ΔG^* can be ruled out.

Acknowledgment. We thank the Dirección General de Investigación Científica y Técnica (Grant PB92-0982-C) and the Fonds der Chemischen Industrie for financial support.

Supporting Information Available: Two X-ray crystallographic files, in CIF format, are available. Access information is given on any current masthead page.

IC970367D